Deuterium NMR Studies of Local Motions of Benzene Adsorbed on Ca-Montmorillonite

Jincheng Xiong and Gary E. Maciel*

Department of Chemistry, Colorado State University, Fort Collins, Colorado 80523-1872

Received: March 8, 1999; In Final Form: April 27, 1999

^{2}H NMR spectra and interpretations are presented on two samples of deuterium-labeled benzene that have been adsorbed on a major soil component, Ca-montmorillonite clay. Spectra were obtained on the samples with two different benzene loading levels over a wide temperature range and using two values of the quadrupolar echo delay period. Computer simulations of line shapes resulting from various forms of local motion of C−^{2}H moieties provide useful guidelines for interpreting the experimental results. The results suggest that absorbed benzene molecules first form π-complexes with Ca^{2+} in the interlayer space of the clay with an adsorption enthalpy of 42 ± 4 kJ/mol at temperatures at or below −75 °C. The adsorbed molecules undergo small-angle wobbling of the C6 axis accompanied by rapid discrete jumps about the C6 axis. At higher temperatures, benzene molecules start to perform large-angle wobbling of the C6 axis with extremely fast jumps around the axis, and eventually desorb from Ca^{2+} to tumble freely in the interlayer space of the clay. The enthalpy and entropy changes between different motional states were obtained from the variable temperature studies. The activation energies of relevant molecular motions were also estimated. This approach is attractive for elucidation of the detailed motional behaviors of organic pollutants adsorbed in soil.

Introduction

For facilitating an accurate prediction of the fates of organic pollutants in the environment (e.g., long-term sequestering, chemical transformation, complexation, release to groundwater, etc.), or the design of effective remediation strategies, it is important to have a fundamental knowledge of the chemical−physical behaviors of such species in soil/groundwater systems. One potentially valuable aspect of understanding this fundamental behavior and, we believe, a valuable property for characterizing the environmental fate of an organic pollutant is the detailed nature of local mobility/motion manifested by the pollutant species adsorbed in the soil system. A pollutant species that interacts strongly with certain regions of a clay will be expected to manifest a more constrained local mobility than if the same species were not interacting at all with "solid" soil substrates, e.g., if it were in a nonaqueous-phase liquid (NAPL) pool. An intermediate local motion/mobility would be expected for a pollutant species that loosely interacts in a physiosorbed manner with a solid component in soil, e.g., a silica or some other mineral system.

The study reported here focuses on one pollutant species, benzene, which has been identified by the Department of Energy as a major soil/groundwater pollutant,[1] and one common type of soil component, Ca-montmorillonite. This study is part of a long-range study of local motion/mobility of pollutant species in soil systems. One might hope that, if the local pollutant motion in a sample of pollutant adsorbed on a whole soil can be recognized as resembling that of the same pollutant adsorbed on one type of major soil component (e.g., clay, silica, humic acid, fulvic acid, humin), then perhaps this recognition will provide a strong indication of the specific component(s) in a complex soil in which a specific pollutant is concentrated.

The formation of chemisorbed surface complexes in benzene/clay systems has been studied by a variety of techniques, including UV−visible, vibrational, and ESR spectroscopies.[2−10] The formation of benzene-based polymers has been observed in these studies, especially in the presence of Cu^{2+}-exchanged forms of the clays. Hinedi and co-workers[9] have reported a FTIR and ^{13}C NMR study of benzene adsorbed on Cu^{2+}-montmorillonite; in that study the former technique provided much more useful information than did the latter, probably because of the influence of paramagnetic centers, e.g., Cu^{2+} sites. In the present study, the emphasis has been entirely on studying local molecular motions, rather than the formation of chemisorbed species in which the carbon−carbon framework is altered. The technique on which this study is based is ^{2}H NMR. An earlier stage of some aspects of this work was included in a survey paper published elsewhere.[11]

^{2}H NMR line shapes have long been recognized as providing a powerful method for elucidating the detailed nature of local mobility of the C−D ≡ C−^{2}H bond in a chemical species with the required ^{2}H labeling.[11−19] In the first-order perturbation regime, the nuclear electric quadrupole effect is given by eq 1:

$$\nu_Q = \pm \frac{3}{8}\frac{e^2qQ}{h}(3\cos^2\theta - 1 - \eta\sin^2\theta\cos 2\psi) \quad (1)$$

where eQ is the "nuclear electric quadrupole moment" (a fixed property of the ^{2}H nuclide), $eq \equiv (\partial^2V/\partial Z^2)_0$ is a property of the local electric field environment in which the ^{2}H nucleus is situated (**V** is the so-called electric field gradient tensor in its principal axis system, X, Y, Z, eq being its largest component), and $\eta \equiv \{(\partial^2V/\partial X^2)_0 - (\partial^2V/\partial Y^2)_0\}/(eq)$ is called the asymmetry parameter. In eq 1, θ is the angle between the Z axis and the direction (z) of the static magnetic field ($\mathbf{B_0}$), and ψ is a second angle relating the two relevant axis systems (x, y, z and X, Y, Z). The quantity e^2qQ/h is often denoted by Q_{CC}.

The factor, $[3\cos^2\theta - 1 - \eta\sin^2\theta\cos^2\phi]$, is summed over all initial orientations and averaged over all transient orientations if the molecule is in motion. The two resonance positions defined by the ± in eq 1 correspond to $\Delta m = -1 \leftrightarrow 0$ and $\Delta m = 0 \leftrightarrow 1$, for each (θ, ϕ) combination. Following the

10.1021/jp990813d CCC: $18.00
Published on Web 06/11/1999

common assumption that the static electric field gradient tensor relevant to the C−^{2}H unit in an organic species is axially symmetric ($\eta = 0$), eq 1 yields the simple form shown in eq 2.

$$\nu_Q = \pm \frac{3}{8} \frac{e^2qQ}{h} (3 \cos^2 \theta - 1) \qquad (2)$$

For a powder or amorphous sample consisting of randomly oriented, static components, the observed ^{2}H NMR pattern has a contribution from each crystallite orientation and (each value of θ) weighted statistically. The classic "Pake pattern," with a full width of about 250 kHz, is the resulting line shape. Motion can "narrow" this pattern in a manner that depends in exquisite detail on the nature of the motion. The usual ^{2}H NMR strategy for elucidating local C−D motion is to compare experimentally determined ^{2}H line shapes with patterns that are simulated by computer calculations. Each such spin-dynamics calculation is based on a specific, assumed motional model, or a composite of motional models.

Experimental Section

The ^{2}H-labeled benzene (C_6D_6) was obtained from Cambridge Isotopes. The Ca-montmorillonite was obtained from the Missouri Clay Repository, Columbia, MO. The samples of C_6D_6 adsorbed on (in) Ca-montmorillonite were prepared by gas-phase adsorption of the C_6D_6 onto the clay in a vacuum line and subsequently sealed in a 5 mm o.d. glass tube for NMR experiments. Prior to this adsorption, the clay had been dried at 50 °C at 10^{-3} Torr for 24 h.

^{2}H NMR spectra were obtained at 92.17 MHz, using a Bruker AM-600 spectrometer that was modified for wide-line ^{2}H NMR spectroscopy by the addition of a 1000-Watt rf amplifier, a home-built high-speed digitizer (1 complex data point/0.5 μs), and a home-built probe. The quadrupole echo technique[16,17] was used to record all ^{2}H spectra, typically in two sets of experiments with pulse spacing periods, $t_q = 40$ μs and $t_q = 100$ μs. The $\pi/2$ pulse width was set as 2.5 μs. A spectral width of 1−2 MHz was typically used to obtain each ^{2}H spectrum. The sample temperature was regulated using home-built variable temperature accessories and a commercial microprocessor-based temperature controller with a stability of ±0.5 °C over the entire temperature range (−125 to +25 °C) employed in this work. The accuracy of sample temperatures was estimated to be within ±0.5 °C.

^{2}H line-shape simulations were based on the MXET1 version of the MXQET program,[19] which was kindly provided by R. R. Vold. The calculated free induction decays were multiplied, prior to Fourier transformation, by the same experimental weighting functions as used in obtaining the experimental spectra. Two C programs were written to increase the efficiency of fitting experimental spectra with simulations. One of programs was used to automatically generate a series of MXET1 input files with multiple input parameters set on a multidimensional grid for searching for the best match. This program also generates a UNIX script for carrying out the calculation in the batch mode. Another program was for generating a macro file to process and plot the simulated spectra automatically using a modified NMR data processing package, FTNMR.[20] The simulations were performed on either an IBM RS/6000 computer or a SGI R5000 workstation.

Results and Discussion

Deuterium NMR spectra obtained on benzene-d_6/Ca-montmorillonite with a benzene loading level of 1.2% (w/w) at a variety of temperatures are shown together with theoretical

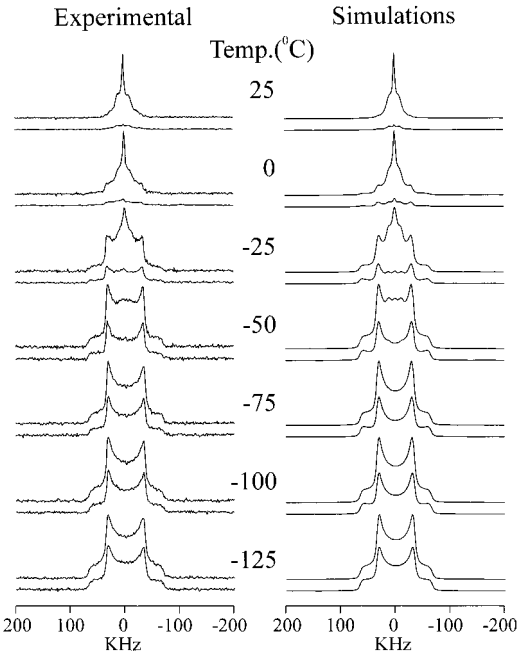

Figure 1. ^{2}H NMR spectra of a sample of C_6D_6 adsorbed on dry Ca-montmorillonite (1.2% w/w loading level) corresponding to a quadrupolar echo delay period (t_q) of 40 μs (upper member of each stacked pair) and 100 μs (lower) and a range of temperatures, as shown: (left side) experimental results; (right side) simulated spectra, obtained as described in the text.

simulations in Figure 1. The experimental line shapes shown in Figure 1, even at the lowest temperature examined (−125 °C), do not correspond to the powder pattern of static molecules, which would be characterized by a Pake-like pattern with a double-horn splitting of 137 kHz. However, all of the experimental line shapes contain a Pake-like component with a double-horn splitting close to half of the static-pattern splitting. This factor-of-two attenuation is apparently due to rapid 60° or 120° jumps of the C−D bond about the C6 axis of the benzene molecule.[11,21,22] A close examination of the double-horn splittings indicates that these splittings decrease slightly with increasing temperatures, from 68.0 kHz at −125 °C down to 64.8 kHz at 25 °C.

The apparent reduction of the quadrupole coupling constant can be attributed to a rapid "wobble" motion of a benzene ring's normal (C6) axis.[21,22] This "wobble" motion can be modeled in the simulation by letting the C6 axis wander rapidly within a cone of half-angle ϕ. If the reorientation of the C6 axis within the cone is *uniform*, the double-horn splitting will be reduced by a factor of $\cos[\phi(1 + \cos \phi)/2]$.[21] In this case, the cone half-angle changes from 5.5° at −125 °C up to 15° at 25 °C. However, if we assume that the C6 axis moves around only the surface of a cone (a *nonuniform* sampling of the volume of the cone), the factor of the splitting reduction is instead $(3 \cos^2 \phi - 1)/2$, which yields the cone half-angles of 3.9° at −125 °C and 11° at 25 °C. The approximate range of the cone half-angle at any particular temperature can be determined from these two limiting cases.

Close examination of the experimental line shapes suggests that the uniform reorientation of the C6 axis *within* a cone is a better model. In practical simulations, we used a pseudouniform 10-site model with the possible orientations of the C6 axis uniformly distributed within a cone. Specifically, in this model there is one "site" with the C6 axis pointing along the center of a cone, three equally spaced "sites" with the C6 axis at an angle of $\phi/2$ with respect to the line pointing to the center of the cone,

TABLE 1: Results of Simulations for ^{2}H NMR Spectra of 1.2% C_6D_6/Ca-montmorillonite Sample

	small-angle wobble (SAW)					large-angle wobble (LAW)			isotropic reorientation	
temp (°C)	P_S (%)[a]	ϕ (deg)[b]	$10^{-4}\,k_{sw}$ (s^{-1})[c]	$10^{-6}\,k_{swn}$ (s^{-1})[d]	$10^{-7}\,k_j$ (s^{-1})[c]	P_L (%)[a]	ϕ (deg)[b]	$10^{-5}\,k_{lm}$ ($s-1$)[e]	P_I (%)[a]	$10^{-5}\,k_{iso}$ (s^{-1})[f]
25	3	12.5	4.0	3.8	2.2	49	54	1.8	48	4.6
0	18	12.5	4.0	3.8	2.2	55	53	1.8	27	6.0
−25	43	10	4.0	3.0	2.2	43	51	1.8	14	7.0
−50	72	9.5	5.5	3.8	2.2	25	51	1.8	3	7.0
−75	100	9	5.5	3.9	2.2					
−100	100	7	4.0	2.1	2.2					
−125	100	4	2.3	0.69	2.2					

[a] P_S, P_L, and P_I are percentages of benzene in SAW, LAW, and IR states, respectively. Estimated uncertainty: ±7% of the number given, except for the value 3%, where it is ±20% of the value given. [b] ϕ is the half-angle of the cone. Estimated uncertainty: ±0.5°. [c] k_{sw} and k_j are site-jump rates of small-angle wobble motion of the C6 axis (10-site wobble in a cone model) and accompanying jump motion about the C6 axis (3-site jump model), respectively. Estimated uncertainty: ±10% of the number given. [d] k_{swn} is the "normalized" wobbling rate as defined in the text. Estimated uncertainty: ±10% of the number given. [e] k_{lw} is site-jump rate of large-angle wobble motion of the C6 axis. Estimated uncertainty: ±10% of the number given. [f] k_{iso} is the site-jump rate of isotropic reorientation of the C_6 axis, as modeled with the 14-site cube model. Estimated uncertainty: ±10% of the number given.

and six equally spaced orientations with the C6 axis at an angle of ϕ relative to the line pointing along the center of the cone. All 10 sites (orientations) were allowed to exchange with each other in the simulation. We also tried simulations with a 19-site model similar to the 10-site model just described. As these two models yielded essentially the same line shapes, we used the 10-site model for C6 axis "wobble" motion in this work (e.g., the simulations shown in Figure 1) to reduce the computation time.

At temperatures between −125 and −75 °C, the experimental deuterium spectra can be simulated with only one composite motion, in which the benzene molecule jumps about its C6 axis while the C6 axis wanders within a cone at the same time. The 10-site model for the C6-axis wobble motion described above and a 3-site model for benzene jump motion about the C6 axis were used in the simulations. The combination of the two resulted in a 30-site model for this multiple-axis composite motion.

We also tried a 6-site nearest-neighbor jump model to represent the discrete jumps about the C6 axis. On the basis of our simulations, and previous work from others, there are apparently no appreciable differences in simulated line shapes between 6-site and 3-site discrete-jump models.[20] Using 3-site jumps instead of 6-site jumps in the two-axis wobble-jump composite motional model reduces the total number of sites from 60 to 30, which reduces computational time by more than a factor of 4. We chose a large-angle discrete jump model instead of a small-step diffusive jump model, because benzene molecules execute the same large angle jumps about their C6 axis in pure solid benzene and in cages of a variety of clathrates.[21,22] More importantly, we can simulate the experimental line shapes very well with this model in the intermediate motional regime.

The results from the simulations are listed in Table 1. To compare wobbling rates with different cone half-angles, the rate k_w should be "normalized" in an appropriate way.[11] For this purpose, we use an "average" site-jump rate k_{wn} as the rate for a total angular excursion by one radian; i.e., $k_{wn} = k_w(\sum_i|\theta_i|)$, where the sum of jump angles, $\sum_i|\theta_i|$, is over all the stepwise jumps that occur during the period, $1/k_w$. For the 10-site model of wobble motion in a cone, we define $k_{wn} = k_w(15\phi/2)$, where ϕ is the cone-half angle. While this may not be the most rigorous way to "normalize" the site-jump rate, it can be easily computed from k_w and also provides appropriate comparisons of wobbling rates with different cone-half angles. As we can see from the Table 1, the frequency of jump motion about the C6 axis is constant, but both the frequency and cone half-angle of wobble motion increases significantly with increasing temperatures due to thermal activation.

At temperatures at or above −50 °C, we start to see more components in the ^{2}H line shapes due to additional types of motion in the benzene-d_6/Ca-montmorillonite system. One can see very clearly that there are at least two additional, distinctively different components in the ^{2}H NMR line shapes obtained at temperatures of 25, 0, and −25 °C. This suggest that there are at least three types of motions that do not exchange rapidly with each other on the NMR time scale. The central narrow line component can be simulated with a model in which the benzene molecule executes extremely rapid jump motion about its C6 axis while the C6 axis undergoes isotropic diffusional reorientation. The extremely rapid C6 jump motion is simulated with an effective Q_{CC} of half of its static-state value.

Although isotropic reorientation motion has often been observed in experimentally determined wide-line deuterium NMR line shapes, this type of motion has rarely been modeled in simulations for intermediate correlation times. However, there are at least three important reasons for establishing appropriate models to simulate this type of motion. First, isotropic reorientational motion is one of most common types of motions, which occurs either as a stand-alone type of motion, or as part of composite types of cooperative motions, such as multiple-axis motion with one axis as isotropic reorientation, or exchange motion with one of the components undergoing isotropic reorientation. Second, the rate of isotropic reorientation, which is a byproduct of a simulation, is an important parameter for studying the molecular dynamics of a system. Third, counting the number of deuterons that experience different types of motions in a system requires simulations of all of the types of motions present in the system, because the integrated intensity associated with each line shape depends strongly on the correlation time(s) of the corresponding dynamic processes. One cannot simply use integrated areas for spin counting of deuterons, if the motion is in an "intermediate" range.

Recently, we proposed and used a 32-site icosahedron model for simulating line shapes due to isotropic reorientation.[11] In this model, the C−D vector reorients among 32 orientations (all-site exchange) corresponding to the 32 lines between the center of an icosahedron and its 20 face centers and 12 vertexes.[11] To reduce the computation time in the work presented here, we used a simplified 14-site model for isotropic reorientation, in which the 14 C−D orientations correspond to the 14 lines between the center of cube and its 6 face centers and 8 vertexes. For the range of correlation times involved in the simulations presented in this work, both models work equally well.

An additional component in the ^{2}H NMR line shapes shown for the higher temperatures in Figure 1 shows a scaled Pake-

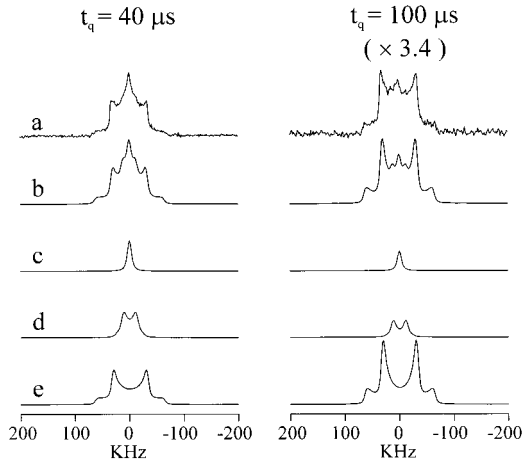

Figure 2. ^{2}H NMR spectra of a sample of C_6D_6 adsorbed on dry Ca-montmorillonite (1.2% w/w/loading level) at −25 °C, corresponding to quadrupolar echo delay periods of 40 μs (left) and 100 μs (right): (a) experimental spectrum; (b) simulated spectrum (sum of c + d + e); (c, d, e) contributions to the simulated spectrum from components with small-angle wobble, large-angle wobble, and isotropic reorientation, respectively. Spectra and contributions for t_q = 100 μs have been vertically scaled by 3.4.

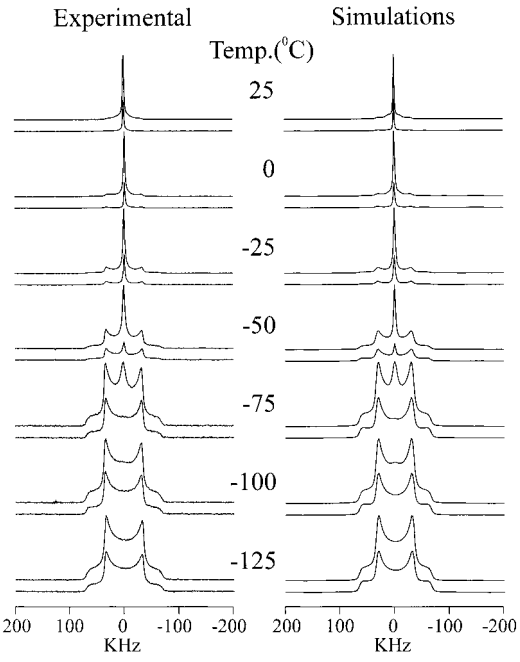

Figure 3. ^{2}H NMR spectra of a sample of C_6D_6 adsorbed on dry Ca-montmorillonite (3.9% w/w loading level) corresponding to a quadrupolar echo delay period (t_q) of 40 μs (upper member of each stacked pair) and 100 μs (lower) and a range of temperatures, as shown: (left side) experimental results; (right side) simulated spectra, obtained as described in the text.

like pattern with a horn splitting between 21 and 25 kHz; this component can be modeled as resulting from a wobble motion of the C6 axis within a cone having a large cone angle, accompanied by extremely fast rotational jumps of the benzene molecule around its C6 axis (simulated with Q_{CC} equal to half of the static case). By comparison with the experimental ^{2}H patterns, the cone half-angle can be estimated as between 65° and 61°, if one assumes a uniform reorientational motion within the cone. If the C6 axis reorientation is confined to the surface of the cone ("nonuniform" motion), the half-angle can be estimated as between 43° and 41°. From simulations based on the 10-site (pseudouniform) model, the cone half-angles are estimated to be between 54° and 51°, halfway between the two limiting cases.

Figure 2 shows experimental and simulated deuterium NMR spectra of a C_6D_6/Ca-montmorillonite sample with a benzene loading level of 1.2% (w/w) at −25 °C. The individual contributions of three motional components due to the three types of composite motion described earlier are clearly illustrated in the figure. For each of these three components the motion is a composite, each with rotation of the benzene molecule about the C6 axis. In one composite, the C6 axis reorients isotropically (Figure 2e). In another composite, the C6 axis reorients in a pseudorandom mode within a cone with a small angle (small angle wobble, <20° cone half-angle). In the third type of composite motion, a large-angle wobble motion (>40° cone half-angle) was employed.

As shown in Figures 1 and 2, excellent fits between experimental spectra and simulations were achieved using the model consisting of the three types of composite molecular motions discussed above. It should be noted that simulating the experimental line shapes obtained with different pulse spacing t_q in quadrupole echo experiments is crucial for validating the molecular dynamic models proposed and for accurately determining parameters of the models. All of the model parameters employed in the simulation shown in Figures 1 and 2 are listed in the Table 1.

In Table 1 one sees that at −50 °C, 25% of the benzene molecules are activated to change from C6-axis small-angle (4° − 13°) wobble (SAW) motion at lower temperature to large-angle (51° − 54°) wobbling (LAW). A small fraction (3%) of the benzene molecules even undergo isotropic reorientation (IR) at −50 °C. The SAW component could be due to benzene molecules adsorbed strongly at the internal surface of the clay, possibly through π types of interactions between benzene and cations in the clay. Benzene molecules of the LAW component should still retain some interaction with adsorption sites in the clay (e.g., cations). However, since the interaction is presumably weaker, one expects that there is more freedom of wobbling of the ring norm in the LAW component. Clearly, the isotropically reorienting benzene molecules are not strongly adsorbed on the clay surface and reorient freely in the interlayer space of the clay.

With increasing temperature, more SAW benzene molecules become activated thermally to the LAW state and eventually to the desorbed IR state. At room temperature, only 3% of the benzene molecules are still adsorbed strongly as the SAW component on the clay surface. About half of the benzene molecules retain weak interactions with adsorption sites on clay in the LAW state. Roughly another half are desorbed from the surface and reorient freely within the interlayer space of the clay (IR state). One interesting result shown in Table 1 is that the reorientation rate of the IR component decreases slightly, but significantly with increasing temperature. This could be due to a higher energy barrier for isotropic reorientation at higher temperature, since more strong-adsorption sites in the clay are available, with some of the benzene molecules desorbed. Also, the interlayer space is more crowded by the much higher fraction of the IR component.

To check how the loading level would affect molecular dynamics of benzene in the Ca-montmorillonite, we carried out deuterium NMR experiments on a sample with a benzene loading level of 3.9% (w/w). The experimental spectra and simulations for this sample are shown in Figure 3. The parameters obtained from the simulations of the experimental spectra are listed in Table 2. We also achieved excellent

TABLE 2: Results of Simulations for ^{2}H NMR Spectra of 3.9% C_6D_6/Ca-montmorillonite Sample

	small-angle wobble (SAW)					large-angle wobble (LAW)			isotropic reorientation	
temp (°C)	P_S (%)[a]	ϕ (deg)[b]	10^{-4} k_{sw} (s^{-1})[c]	k_{swn} (s^{-1})[d]	10^{-7} k_j (s^{-1})[c]	P_L (%)[a]	ϕ (deg)[b]	10^{-5} k_{lm} ($s-1$)[e]	P_I (%)[a]	k_{iso} (s^{-1})[f]
25	18	17.5	6.0	7.9×10^6	2.2	51	53	1.8	31	1.8×10^6
0	23	13	4.0	3.9×10^6	2.2	30	54	1.8	47	1.4×10^6
−25	47	9.5	4.0	2.9×10^6	2.2				53	1.6×10^6
−50	68	7.5	4.5	2.5×10^6	2.2				32	8.5×10^5
−75	70	7.5	4.5	2.5×10^6	2.2				30	4.2×10^5
−100	74	7	4.0	2.1×10^6	2.2				26	2.5×10^5
−125	100	4	1.7	5.1×10^5	2.0					

[a] P_S, P_L, and P_I are percentages of benzene in SAW, LAW, and IR states, respectively. Estimated uncertainty: ±7% of the number given. [b] ϕ and k_j are site-jump rates of small-angle wobble motion of the C6 axis (10-site wobble in a cone model) and accompanying jump motion about the C6 axis (3-site jump model), respectively. Estimated uncertainty: ±10% of the number given. [d] k_{swn} is the "normalized" wobbling rate as defined in the text. Estimated uncertainty: ±10% of the number given. [e] k_{lw} is site-jump rate of large-angle wobble motion of the C6 axis. Estimated uncertainty: ±10% of the number given. [f] k_{iso} is the site-jump rate of isotropic reorientation of the C_6 axis, as modeled with the 14-site cube model. Estimated uncertainty: ±10% of the number given.

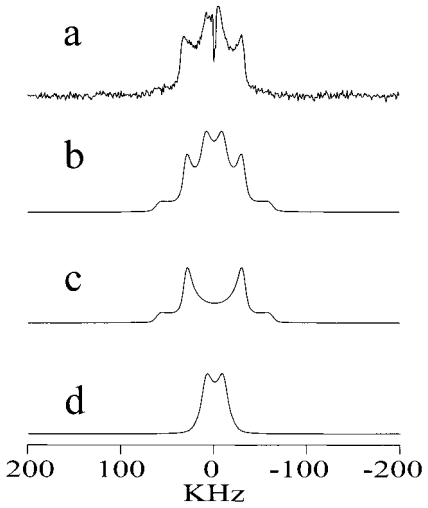

Figure 4. ^{2}H NMR spectrum of a sample of C_6D_6 adsorbed on dry Ca-montmorillonite (3.9% w/w/loading level) at 0 °C, corresponding to a quadrupolar echo delay period of 40 μs: (a) experimental spectrum minus the sharp center contribution due to the isotropically reorienting component; (b) simulated spectrum (sum of c + d); (c, d) contributions to the simulated spectrum from components with small-angle wobble and large-angle wobble, respectively.

agreement between the experimental spectra and simulations based on molecular dynamics models discussed below.

The spectrum obtained at −125 °C contains only one SAW component with a cone half-angle of 4°, similar to the one for a 1.2% loading level. However, we see additional components at a temperature as low as −100 °C. At temperatures between −100 and −25 °C, the experimental line shapes can be fitted with two components, a SAW component and an IR component, instead of the three components found necessary for the sample with a 1.2% loading level. Since the narrow IR component dominates the spectra, especially at relatively high temperatures, it is difficult to determine if there is an additional LAW component, even with vertically expanded spectra. In a previous survey paper,[11] we used only two components, SAW and IR, to simulate the experimental spectra of this sample over the entire temperature range (−125 to +25 °C). We found later that an additional component can, however, be identified relatively easily in this case by subtracting the dominant, narrow Lorentzian line due to the IR component from the original spectrum. An example of this spectral decomposition is shown in Figure 4, in which the LAW component with a double-horn splitting about 21 kHz was successfully identified and simulated for the 0 °C spectrum of the 3.9% C_6D_6/Ca-montmorillonite sample. From this analysis, it turns out that as much as 30% of the benzene molecules are in the LAW state at 0 °C.

The SAW component of the 3.9% C_6D_6/Ca-montmorillonite sample shows a temperature dependence that is similar to that of the sample with a 1.2% loading level. The rate of rotational jumps about the C6 axis is independent of temperature, but the wobbling rate of the C6 axis becomes larger at higher temperature. The rate of isotropic reorientation of the IR component is much higher in the 3.9% C_6D_6/clay sample than that of the 1.2% C_6D_6/clay sample and increases with increasing temperature. This may be due to the fact that most of the strong absorption sites in the clay are already saturated with benzene at a loading level of 3.9%, so that the major interactions for desorbed molecules are van der Waals interactions among themselves instead of relatively strong benzene−clay interactions. This would also explain differences between the two loading levels of interconversion among the three types of composite motions as the temperature is varied. At a loading level of 1.2%, most benzene molecules are converted from SAW to LAW first as the temperature is increased and then progressively to IR at higher temperatures. This is because most of the benzene molecules are strongly bound to the clay surface at a 1.2% loading level. Thermal activation makes some of the molecules in relatively weak adsorption sites start to execute a large-angle wobble motion of the ring normal, eventually leading to desorption from the clay to tumble isotropically within the interlayer space. This view also suggests that in the benzene−clay system, there are π-type complexes at the adsorption sites. At a loading level of 3.9%, a significant fraction of the benzene molecules are not bound directly to the surface of the clay, even at low temperatures and could be adsorbed on a benzene layer of molecules that is bound directly to the surface to form adsorption multilayers. To be desorbed to tumble freely in the interlayer space of the clay, these molecules need only the energy to overcome van der Waals interactions among themselves.

From the simulation results listed in Table 2, one can see that in the 3.9% C_6D_6/clay sample 26% of the benzene molecules are already converted from SAW to IR at a temperature as low as −100 °C. And, the fraction of IR components only increases slightly from 26% to 32% until the temperature reaches −25 °C. Consistent with the results for the 1.2% loading level, −25 °C seems to be a threshold temperature for desorbing benzene molecules bound on the clay surface into the interlayer space of the clay. This suggests that a lower limit of adsorption energy for benzene or Ca-montmorillonite is around kT at −25 °C, which is 2.1 kJ/mol. The van der Waals energy of interaction among benzene molecules within an adsorption multilayer on

the clay surface should be roughly the value of kT at −100 °C, or 1.4 kJ/mol. As only about 70% of the benzene molecules are bound directly to the surface of the 3.9% C_6D_6/Ca-montmorillonite sample, the maximum loading level for benzene to form a single adsorption layer on the surface of Ca-montmorillonite is about (70% × 3.9%), or 2.7%, which is equivalent to 3.3×10^{-4} mol of benzene/g of clay. According to the elementary analysis data provided with the clay, the amount of Ca^{2+} in the Ca-montmorillonite is 2.9×10^{-4} mol/g, which is equal within experimental error to the amount of benzene molecules that would be required for forming the first strong (1:1) adsorption layer in the clay. This result suggests that the strong benzene−clay interaction is due to formation of 1:1 π complexes between Ca^{2+} and benzene.

The simulation parameters summarized in Figure 1, Figure 3, Table 1, and Table 2 provide estimates of populations and rate constants of C−D moieties executing three different types of motions over a range of temperature from −125 to 25 °C. From the simulation parameters required to fit the experimental spectra over this temperature range, one obtains important information on the temperature dependence of these motional rate constants and of the equilibrium constants among the C−D containing species in the various motional states. The activation energy of a specific type of motion, and the corresponding enthalpy and entropy changes from one motional state to another, can thus be estimated.

As the C_6D_6/Ca-montmorillonite system is not a simple system that experiences only one type of molecular motion, raising the temperature can accelerate a specific type of motion and/or increase the fraction of C−D moieties in a relatively high energy motional state. To apply the Arrhenius equation for estimating the activation energy of a specific type of motion, the interpretation is less complex if one chooses a temperature range in which the fractions of different components in a system do not change dramatically. For example, in the sample with a loading level of 3.9%, rate constants obtained between −100 and −50 °C are good for estimating the activation energy of isotropic reorientation, which is 8.8 kJ/mol. Similarly, we can evaluate the activation energy of small-angle wobbling motion (k_w) in the sample with a 1.2% benzene loading level as 8.3 kJ/mol for temperatures between −125 and −75 °C.

It would be very interesting to obtain estimates of the adsorption enthalpy and entropy of benzene on Ca-montmorillonite. The sample with a 1.2% loading level should be a good system for this purpose, as all the benzene molecules are bound to strong adsorption sites, presumably Ca^{2+}, in the clay, at temperatures below −75 °C. The complication due to multilayer adsorption in the sample with a 3.9% loading level is not present in the 1.2% case. At temperatures above −50 °C, three motional states, SAW, LAW, and IR, coexist in the C_6D_6/Ca-montmorillonite system with a 1.2% loading level, as shown in Table 1. The equilibrium constants among the three states can be calculated from the corresponding ratios of fractional populations among the different states. Plots of ln K vs $1/T$ for the three equilibria, SAW ⇄ LAW, LAW ⇄ IR, and SAW ⇄ IR, are shown in Figure 5a. Corresponding least-squares linear-line fits to the data using the van't Hoff equation, $d(\ln K)/d(1/T) = -\Delta H°/R$, are also shown in the figure. The enthalpies and entropies estimated from this analysis are listed in Table 3 and are represented in Figure 5b. Values of $\Delta H°_{SL}$, $\Delta S°_{SL}$, $\Delta H°_{LI}$, $\Delta S°_{LI}$, and $\Delta H°_{SI}$, and $\Delta S°_{SI}$ were obtained *independently* from corresponding "ln K vs $1/T$" curves, as shown in Figure 5; yet, there is a perfect agreement in the relationships $\Delta H°_{SI} = \Delta H°_{SL} + \Delta H°_{LI}$, and $\Delta S°_{SI} = \Delta S°_{SL} + \Delta S°_{LI}$, as seen from the numbers given in Table 3. The adsorption enthalpy $\Delta H°_{SI}$ and entropy $\Delta S°_{SI}$ (relative to isotropically reorienting benzene) for benzene and strong adsorption sites in the clay were estimated in this manner to be 42 ± 4 kJ/mol and 0.16 ± 0.01 (kJ/mol)/K, respectively. Such a high adsorption energy further supports the view that the strong benzene−clay interaction is due to formation of π complexes between Ca^{2+} and benzene.

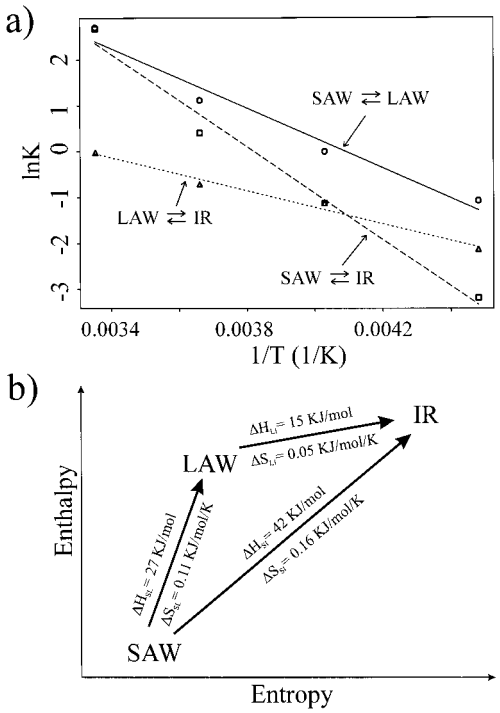

Figure 5. (a) Plots of ln K vs $1/T$ for the three indicated equilibria in the 1.2% C_6D_6/Ca-montmorillonite sample at temperatures between −50 and +25 °C. (b) Pictorial representation of the three motional states to which the three equilibria indicated in Figure 5a correspond, showing thermodynamic parameters; *not* to scale.

TABLE 3: Adsorption Enthalpy Changes ($\Delta H°$) and Entropy Changes ($\Delta S°$) of Benzene among Three Different Motional States: Small-Angle Wobbling (SAW), Large-Angle Wobbling (LAW), and Isotropic Reorientation (IR)[a]

	SAW ⇄ LAW	LAW ⇄ IR	SAW ⇄ IR
$\Delta H°$ (kJ/mol)	27 ± 3	15 ± 1	42 ± 4
$\Delta S°$ [(kJ/mol)K]	0.11 ± 0.01	0.050 ± 0.005	0.16 ± 0.01

[a] Estimated from the temperature dependence of equilibrium constants derived from the simulations (Tables 1 and 2).

The temperature dependence of the equilibrium constants estimated for the SAW ⇄ IR equilibrium between −100 and −50 °C in the sample with a 3.9% loading level provides additional interesting information on the adsorption energy of excess benzene molecules that are weakly adsorbed in the clay. The adsorption enthalpy and entropy (relative to isotropically reorienting benzene) were estimated as 1.9 ± 0.3 kJ/mol and 2.4 ± 1.2 (J/mol)/K, respectively. This adsorption energy is in agreement with what was estimated above as roughly kT at −100 °C (1.4 kJ/mol).

Conclusions

The ^2H NMR spectra and corresponding line-shape simulations presented in this paper have provided new insight into the molecular motion of benzene adsorbed on Ca-montmorillonite. At a benzene loading level below 2.7% w/w and temperatures between −75 and −125 °C, benzene molecules

appear to form π complexes with Ca^{2+} in the clay and undergo small-angle wobbling of the C6 axis, accompanied by rapid, discrete jumps around the C6 axis. The adsorption of this species is quite strong, with an adsorption enthalpy of 42 ± 4 kJ/mol (relative to isotropically reorienting benzene). At temperatures at and above -50 °C, some benzene molecules are thermally activated to perform large-angle wobbling of the C6 axis, along with extremely fast jumps about the C6 axis. The energy of benzene molecules performing large-angle wobbling motion is 27 ± 3 kJ/mol higher than those undergoing small-angle wobbling. And, at a temperature of -50 °C or above, a small fraction of the benzene molecules start to desorb from Ca^{2+} and tumble freely in the interlayer space of the clay. The fractions of molecules undergoing large-angle wobbling and isotropic reorientation increase with increasing temperature. With a benzene loading level above 2.7% w/w, excess benzene molecules are adsorbed weakly in the clay, with an adsorption energy of 1.9 ± 0.3 kJ/mol (relative to isotropically reorienting benzene) and desorb from the clay to undergo isotropic reorientation even at temperatures as low as -100 °C.

The combination of variable-temperature wide-line ^2H NMR experiments and computer line-shape simulations constitutes an extremely powerful tool for elucidating details of local motions of organic pollutants adsorbed on a soil component, as demonstrated in this paper. This approach, which can be implemented straightforwardly with widely available equipment and computers, shows great promise for examining an extremely important aspect of the fundamental behaviors of pollutant species adsorbed in soils.

Acknowledgment. The authors gratefully acknowledge support of this work by DOE grant No. DE-FG-03-95ER14558 and R. R. Vold for providing the simulation program, MXET1. We also thank Dr. Jane Yang for preparing the samples.

References and Notes

(1) Riley, R. G.; Zachara, J. M.; Wobber, F. J. *Chemical Contaminants on DOE Lands and Selection of Contaminant Mixtures for Subsurface Science Research*; U.S. Department of Energy, Office of Energy Research, Subsurface Science Program: Washington, DC, 20585, April, 1992.
(2) Pinnavaia, T. J.; Mortland, M. M. *J. Phys. Chem.* **1971**, *75*, 3957.
(3) Van de Poel, D.; Cloos, P.; Helsen, J.; Jannini, E. *Bull. Gr. Fr. Agr.* **1973**, *25*, 115.
(4) Soma, Y., Soma, M. and Harada, I., *J. Phys. Chem.* **1984**, *88*, 3034.
(5) Doner, H. E. and Mortland, M. M., *Science* **1969**, *166*, 1406.
(6) Eastman, M. P., Patterson, D. E. and Pannell, K. H., *Clays Clay Miner.* **1984**, *32*, 327.
(7) Walter, D., Saehr, D. and Wey, R., *Clay Miner.* **1990**, *25*, 343.
(8) Mortland, M. M. and Halloran, L. J., *Soil Sci. Soc. Am. J.* **1976**, *40*, 367.
(9) Stoessel, F., Guth, J. L. and Rey, J., *Clay Minerol* **1977**, *12*, 255.
(10) Hinedi, Z. R., Johnston, C. T. and Erickson, C., *Clays Clay Miner.* **1993**, *41*, 87.
(11) Xiong, J., Lock, H., Chuang, I.-S, Keeler, C. and Maciel, G. E., *Environ. Sci. Technol.*, in press.
(12) Spiess, H. *Adv. Polym. Sci.* **1985**, *66*, 23.
(13) Jelinski, L. W. *Annu. Rev. Mater. Sci.* **1985**, *15*, 359.
(14) Barbara, T., Greenfield, M. S., Vold, R. L., Vold, R. R. *J. Magn. Reson.* **1986**, *68*, 311.
(15) Hirschinger, J., English, A. D. *J. Magn. Reson.* **1989**, *85*, 542.
(16) Jurkiewicz, A., Frye, J. S., Maciel, G. E. *Fuel* **1990**, *69*, 1507.
(17) Davis, J. H., Jeffrey, K. R., Bloom, M., Valic, M. I., Higgs, T. P. *Chem. Phys. Lett.* **1976**, *42*, 390.
(18) Boden, N., Clark, L. D., Hanlon, S. M., Mortimer, M. *Faraday Symp. Chem. Soc.* **1978**, 109.
(19) Greenfield, M. S., Ronemus, A. D., Vold, R. L., Vold, R. R., Ellis, P. D., Raidy, T. E. *J. Magn. Reson.* **1987**, *72*, 89−107.
(20) Hare Research, Inc.
(21) Ok, J. H., Vold, R. R., Vold, R. L., Etter, M. C. *J. Phys. Chem.* **1989**, *93*, 7618−7624.
(22) Ronemus, A. D., Vold, R. R., Vold, R. L., *J. Chem. Soc., Fraday Trans. 1*, **1988**, *84*, 3761−3766.